INTERNATIONAL JOURNAL OF CHEMICAL REACTOR ENGINEERING

Volume 1 2003 *Article* A21

Bubble Size Reduction in a Fluidized Bed by Electric Fields

Flip Kleijn van Willigen* J. Ruud van Ommen†

Jan van Turnhout‡ Cor van den Bleek**

*Delft University of Technology, F.KleijnvanWilligen@TNW.TUDelft.Nl

†Delft University of Technology, j.r.vanommen@tudelft.nl

‡Delft University of Technology, J.vanTurnhout@TNW.TUDelft.Nl

**Delft University of Technology, C.M.vandenBleek@TNW.TUDelft.Nl

ISSN 1542-6580

Copyright ©2003 by the authors.

All rights reserved.

Brought to you by | Bibliotheek TU Delft
Authenticated | 172.16.1.226
Download Date | 8/14/12 8:51 AM

Bubble Size Reduction in a Fluidized Bed by Electric Fields

Flip Kleijn van Willigen, J. Ruud van Ommen, Jan van Turnhout, and Cor van den Bleek

Abstract

The reduction of the size of bubbles can improve both selectivity and conversion in gas-solid fluidized beds. Results are reported of the reduction of bubble size by the application of electric fields to uncharged, polarizable particles in fluidized beds. It is shown how average bubble diameters can be drastically reduced, with little change of the bed expansion. A literature review shows that to maintain smooth fluidization, electric fields in the direction of the gas flow, with a relatively low alternating frequency, are optimal. To measure average bubble diameters, a spectral decomposition technique of pressure fluctuation time series is used. Using this method, based on non-intrusive measurements, a characteristic length scale for bubble diameters can be found. It is shown experimentally, using video analysis, that this length scale is of constant proportionality for a given bed material and bed dimensions. The proportionality of the length scale to bubble diameter is independent of measuring height or gas velocity. With this, we have a tool for measuring bubble diameters in both 2-D and 3-D fluidized beds. Electric fields were applied to fluidized beds using thin wire electrodes placed inside the column. Both 2-D and 3-D columns were tested over a range of frequencies and field strengths. For Geldart A glass beads, an optimal range was determined at 5-20 Hz and 400-1600 V/cm fields. The reduction of bubble diameter was measured to be up to 25% for this system. Larger Geldart B glass particles show a larger reduction of bubble diameters - up to 85%. For these particles, the optimal frequency was at a higher range, 20-70 Hz. At higher frequencies (up to 100 Hz), bubble size reduction is less, but still substantial. Experiments in the 3-D column using Geldart A particles show a similar reduction in bubble diameters.

KEYWORDS: Fluidized bed, electric fields, bubble size reduction, polarized particles, pressure fluctuation analysis, video analysis

Brought to you by | Bibliotheek TU Delft
Authenticated | 172.16.1.226
Download Date | 8/14/12 8:51 AM

1. INTRODUCTION

Fluidized beds are quite common in the chemical and process industry, since they have several desirable properties. Their liquid-like behavior and continuous movement of particles allow for good heat transfer and temperature control. However, the appearance of gas bubbles lowers the mass transfer in bubbling fluidized beds. A reduction in bubble size by a factor of four can increase the conversion by as much as 84% (Levenspiel, 2002). Not only the conversion, but also the selectivity will be affected positively (Kaart, 2002). Adaptations have therefore been proposed to reduce the bubble size and increase chemical conversion, selectivity and efficiency.

Baffles and staging are sometimes applied in industrial units, but the effect on the bubble size is often limited. More advanced methods of bubble size reduction have been reported as well: mechanical vibration of the bed (Kwauk, 1992), use of pulsed or fractal feeds (Coppens, 2001), and application of magnetic fields (Rosensweig, 1995, Hristov, 2002). However, the applicability of these methods is restricted by a high energy consumption or by problems associated with their implementation.

In this paper, results are reported of the application of electric fields to fluidized beds with the aim of reducing the bubble size in the bubbling fluidization regime. The fields applied require only a low power input (40-80 Watt per m^3 of fluidized bed. This is three orders less than for magnetic fields (Geuzens, 1985)). Moreover, only small electrodes need to be placed in the bed. The electric fields are applied in such a way that the free movement of particles – the basis for fluidization – is not impaired. Results will be given of the bubble size reduction achieved by applying electric fields of moderate strength (1-10 kV/cm), and low frequency (1-100 Hz).

A technique for determining the bubble size from pressure fluctuations measured in the bed is explored to assess changes in the bubble size both in flat, 2-D columns and in cylindrical, 3-D columns. By applying this technique, we are no longer limited to 2-D systems for visual observation, nor do we have to rely on measuring pressure drop or bed expansion in 3-D columns. A validation is presented of the pressure fluctuation method by using video image analysis.

2. EARLIER WORK

First, we will briefly review previous work on the effect of electric fields on fluidization. Much of this work lacked a sound, quantitative assessment of bubble behavior. Bed expansion and visual observation were often used, but these methods do not allow for a reliable measurement of the bubble size. The review also makes clear that the direction of the electric field, the fact whether an alternating (AC) or a constant (DC) field is used, and the relative humidity of the system are parameters that have a strong impact, because they determine whether or not particle movement is preserved.

The electrical stabilization of fluidized beds is first mentioned in a patent granted to Katz (1967). He describes work on a circular fluidized bed of 10 cm in diameter. The electrodes consisted of a screen on which the fluidized material (glass, $d_p \approx 0.274$ mm) rests, and of a tapered brass rod located above the bed. A potential of 25 to 100 kV DC is placed between the electrodes. The field strength is so high that gas ionization occurs, which results in a non-fluidized bed. The dependence on surface conductivity is indicated. It is claimed that partial ionization of the fluidizing medium is required although this stabilizes the system so much that it collapses into a packed bed.

The first publication about the influence of electric fields on fluidization without gas ionization is by Johnson and Melcher (1975). They described the dynamics of stabilization of fluidized beds of semi-insulating particles. Cross-flow (field lines perpendicular to the gas flow), co-flow (field lines parallel to the flow), and bed suspension are discussed. Johnson et al. used sand particles with a mean diameter of 0.5 mm. The parameter examined most is the particle's conductivity, which is varied by changing the relative humidity of the gas from 8 to 99%. All experiments were done with DC. Examining a column with a square cross-section of 3.82×3.82 cm^2 equipped with electrodes on the column walls (cross-flow fields)

Brought to you by | Bibliotheek TU Delft
Authenticated | 172.16.1.226
Download Date | 8/14/12 8:51 AM

and imposing a field of 2.62 to 9.18 kV/cm, they observed that the bubbles were distorted to fill the cross section of the bed, but that a state of fluidization was retained. At the higher field strengths, the bed became essentially frozen, with channeling of the gas flow. At lower field strengths, it is not clear whether the distorted bubbles passed through the fluidized bed, or whether agglomerates of particles above them suppress the gas voids – as if attempting to fluidize cohesive Geldart C material. At a low relative humidity, they observed a build-up of particles on the electrodes. After 2-10 minutes a thick layer of particles was formed. Frictional charging, which arises due to the long particle relaxation time at low humidities, is blamed for this phenomenon. Again, it is important to recall that the experiments were done with DC. They employed the same column in a co-flow configuration, but now with 0.635 cm square mesh screen electrodes, which allow particles to pass. From the photographs shown, it can be deduced that the setup had six alternating electrodes, spaced 4 cm apart. The photographs also show that the screens have a strong influence on the fluidization: apparently some of the particles are suspended on the screens, resulting effectively in a stack of 5 small fluidized beds (multi-stage fluidized bed). Johnson et al. conclude that with DC fields in co-flow no 'state of fluidization seems to exist whereby particles and field form a rheologically unique continuum'. Between the electrodes strings of particles and little bubbles are seen at high relative humidities, whereas at lower humidities, large voids are created, which lead to frozen sub-beds. In a modified cross-flow set up, they also investigated an electromechanical bed support, using a slit orifice of 0.47 cm to support a 30 cm bed electrically. They conclude that the additional effect of the electric field is small, compared to the role the fluidization gas plays to support the bed.

In a later publication, Dietz and Melcher (1978) compared experimental results of a DC stabilized bed with theoretical calculations. Since a high DC voltage is used, the particles form strings, or are frozen in space. Both the minimum flow required to hold such a bed against a top screen and the minimum flow required to fluidize a stabilized bed were determined. Subsequently, measured shear stresses are compared with calculated ones. They use a simplification of the interparticle model proposed by Colver (2000) described below. The observations apparently corroborate the model, although it should be noted that frozen rather than fluidized beds are considered.

Zahn and Rhee (1984) and Moissis and Zahn (1986) describe experiments that build on Melcher's work. They focus on AC fields, and include the mechanisms of polarization and charge build-up around particle contacts, but they rule out electrostatic charging. Space charge effects were minimized by the use of dry air. These researchers have moved from electrostatic precipitator principles (static agglomeration of particles) to controlling fluidized beds. Stabilization (frozen beds) was no longer the issue – reduction of bubbles was. A stability analysis is included, but the experimental details and comparisons are rather sketchy. Zahn and Rhee state that 'under AC fields it is possible that attracting particles unlock twice each period when the fields go through zero so that the bed retains its fluidity. This small-scale jitter together with gas velocity perturbations may cause enough fluctuations for the particles not to clump together over a range of electric field strengths.' Their statement is in-line with what we will discuss later in this paper.

Wittmann et al. (1987) continued along the line started by Zahn and coworkers – the reduction of bubbles in fluidized systems. In a detailed set of experiments they reported a change in bubble shape towards an ellipsoid under the influence of DC fields. The decrease in bubble velocity indicates that, like in the work of Melcher, DC fields provokes in a strong cohesion of particles in the bed, and a decrease in fluidity. Wittmann (1989) also provides a theoretical analysis of the effect of DC fields on semi-insulating particles with surface conductivity.

Elsdon and Shearer (1977) employed alternating electric fields to increase heat transfer. They use PMMA particles ($d_p \approx 240$ μm), which they allowed to acquire a static charge. They observed that in oscillating fields a maximum rise in heat transfer occurs at about 100 Hz. They also noticed that at lower gas velocities the optimum was not always reached at the highest potential.

Colver et al. (1977, 2000) presented an interparticle force model for a semi-insulating powder in alternating fields, and compared the model to several experimental data. Estimates for relevant characteristic times, as well as for the interparticle forces are given. Based on simple lumped circuit theory, field-frequency trends are predicted. They verify these trends experimentally on the basis of bed

Brought to you by | Bibliotheek TU Delft
Authenticated | 172.16.1.226
Download Date | 8/14/12 8:51 AM

expansion. However, we will show that the measurement of bed expansion is insufficient to determine more subtle changes in bubble size; we therefore applied a pressure fluctuation analysis instead.

3. INTERPARTICLE FORCES

The experiments described later, as well as those reviewed above, are based on the fluidization of semi-insulating particles in a non-conducting gas. In this section, the mechanisms of polarization are outlined. Sometimes reference will be made to the field of electrorheology. Electrorheological fluids are composed of small particles dispersed in non-conducting liquids, in which the flow properties (e.g. viscosity) are altered by applying electric fields. A review of the mechanisms and models has been given by e.g. Parthasarathy and Klingenberg (1996). Although the properties of the continuous phase in electrorheological fluids (liquid, often a non-conducting oil) differ from those of the gas used in fluidization, insight may be gained from the models proposed for particle-particle interaction.

3.1 Polarization

We will first consider the response of particles to an electric field. The particles do not carry a static charge which would result in Coulombic forces, but are polarized by a field-induced charge separation due to their relative dielectric constant $k_p > 1$ (cf. Figure 1a). The molecular dipoles in the particles are oriented by the electric field. This alignment usually occurs much faster than the field oscillation frequencies used in our experiments (0.5-100 Hz). Because the particles are typically not uniformly dispersed, the calculation of the strength of the overall dipole moment becomes quite difficult, even after simplifying the particle dipoles to point dipoles. Approximations have been made and interparticle forces estimated. Such a model, however, cannot explain the frequency and conductivity dependence observed experimentally both in electrorheology and in electric field improved fluidization.

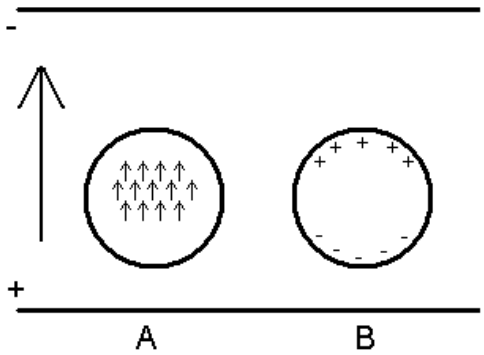

Figure 1. Polarization of particles by an external field. (A) microscopic molecular dipole polarization. (B) macroscopic Maxwell-Wagner polarization by charge accumulation in the surface layer at the gas-solid interface.

The basic point that needs to be addressed is the polarization mechanism. As stated above, the polarization due to molecular dipole orientation reacts virtually instantaneously to field changes, and so this phenomenon cannot explain the observed frequency dependence. Therefore, the intrinsic particle bulk-conductivity and/or the particle surface conductivity (influenced by humidity) play a role in the experiments. The Maxwell-Wagner effect (see e.g. Parthasarathy, 1996) offers the simplest description of the data – it captures the polarization based on the movement of charges to the gas-solid interface owing to a finite conductivity (cf. Figure 1b). The conductivity may stem from both bulk and surface conductivity. The often strong influence of relative humidity on the hydrodynamics in electric fields and the less-than-expected influence of high dielectric constants in electrorheology, make it reasonable to assume that

Brought to you by | Bibliotheek TU Delft
Authenticated | 172.16.1.226
Download Date | 8/14/12 8:51 AM

Maxwell-Wagner polarization by surface conduction is generally the dominant mechanism. The interfacial positive and negative charges then reside in the surface layer.

3.2 Magnitude of Interparticle Forces

After attributing the charge separation in the particle, either to molecular dipole orientation or interfacial Maxwell-Wagner polarization, or to a combination of both, the maximum interparticle force can be calculated. Figure 2 illustrates the interactions between particles in an electric field in two positions. The particle-particle forces are an order of magnitude larger than for simple two dipole-dipole interactions. Chen et al. (1990) used an expansion of spherical harmonics to calculate interparticle forces in infinite chains of dielectric spheres in electrorheological suspensions. They report forces of 10^{-9} N / particle for 70 μm glass beads such as employed in our experiments. The forces calculated by Colver (2000) range from 10^{-10} to 10^{-8} N / particle. The electrical forces are of the order of the drag force and the force of gravity, but they decay quickly as the distance between the particles increases. In other words, the electric force is a relatively short-range attractive or repulsive force.

As the particle diameter increases, the drag and gravity forces grow faster in magnitude than the electric forces (see e.g. Jones, 1995). However, by virtue of the definition of fluidization, the drag and gravity forces balance each other. This allows even small forces to play a significant role in the fluidization. Such small forces are not only the polarization forces described here, but also Van der Waals forces and electrostatic effects (Seville et al., 2000).

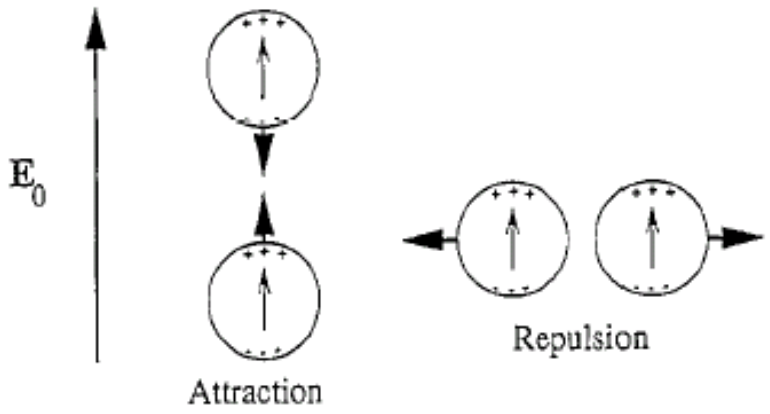

Figure 2. Electric forces between particles polarized in an electric field by the Maxwell-Wagner effect due to the migration of opposite charges provided by the bulk conductivity. Drawing adapted from Parthasarathy et al. (1996).

What does this mean for fluidization in alternating electric fields? The particles will periodically experience a cohesive force in the direction of the field. This attraction force will depend on the frequency and is relatively stronger for smaller particles. The interparticle force, and its cyclic variation, will affect the hydrodynamic behavior of the fluidized bed. Under the right circumstances (force /frequency/direction) the tendency of the particles to form loose agglomerates will decrease the bubble size found in fluidized beds. The field strength must not be so high as to freeze the bed. We will show in section 5 that the range of frequencies that produce optimal bubble size reduction is bounded as well.

Brought to you by | Bibliotheek TU Delft
Authenticated | 172.16.1.226
Download Date | 8/14/12 8:51 AM

4. EXPERIMENTAL

Three types of fluidization experiments were conducted – in three different columns:

- Verification of the pressure fluctuation analysis to determine bubble sizes in a flat 2-D column.
- The influence of electric fields on fluidization in a flat, 2-D column.
- The influence of electric fields on fluidization in a cylindrical, 3-D column.

The 2-D column built to demonstrate that the bubble size can be deduced from pressure fluctuations measured along the side of the column will be described first. This first setup was operated without any electric field applied. A second column was fitted with electrodes and used for experiments on electric field improved fluidization. The 2-D setups will be referred to by their cross-section, 400×15 mm^2 and 200×15 mm^2 respectively. The apparatus with the 3-D column, also equipped with electrodes, will be described last.

4.1 Validation of Pressure Fluctuation Analysis for Determining Bubble Sizes

The correlation between bubble size and the spectral power density analysis was verified in a transparent two-dimensional column with an internal cross-section of 400x15 mm^2. The bed support consists of a porous sintered bronze plate. The settled bed height was 800 mm.

At a height of 10, 200, 400, 600, and 800 mm above the support plate, as well as in the wind box, pressure fluctuations were measured using Kistler piezo-electric pressure transducers, type 7261. The charge from the piezo element was amplified and converted to a voltage using a Kistler amplifier type 5011. The signals were high-pass filtered with a cut-off frequency of 0.16 Hz. The transducers measured the pressure fluctuation relative to the average pressure with an accuracy of 2 Pa, and owing to the high-pass filter, the average of the measured pressure time series is zero. The sensors were connected to the column by 100 mm copper tubes (i.d. 4 mm), which were covered with 40 μm mesh wire gauze at the tips to prevent particles from entering. The probe tips were fitted flush with the sidewalls. The total dead volume of sensor and probe was 2500 mm^3. In the range of frequencies typical for gas-solid fluidized systems (0-50 Hz), no significant distortion of the amplitude or phase of the pressure fluctuations was found (Van Ommen et al., 1999). The data were recorded with a SCADAS II data acquisition system from LMS-Difa. Time series typically consist of 184,320 points, sampled at 400 Hz (approximately 7.5 minutes).

A digital video camera (Sony DCR-TVR130E) was used to film the column. The area of the column under investigation was visible through a 'window' – the rest of the setup was covered to prevent stray light and reflections being recorded. The data were analyzed using Mathworks Matlab, Mathworks Image Analysis Toolbox, and the image analysis package DIPImage (Delft University of Technology). The recorded images were processed and filtered, after which the mean bubble diameter was determined for the first, second, third, and fourth quarter of the settled bed height.

4.2 Bubble Size Reduction in a 2-D Column by Electric Fields

The 2-D electric field equipped column has an internal cross section of 200×15 mm^2. The support consists of a grounded porous sintered steel sieve plate, $\Delta P = 13$ mbar at $U = 1$ cm/s, with a wind box of 300 ml. The walls, made from 6 mm thick transparent Plexiglas, are 700 mm high. The electrodes pass through the bed and consist of a regular wire pattern strung through the column front and rear. The electrodes are alternately, both horizontally and vertically, grounded or connected to a Trek 20/20C high-voltage power supply (Figure 3). The electrodes thus create a quadrupole field with horizontal and vertical components (cf. inset). The nichrome wires have a diameter of 250 μm. The volume density of the wires is about 0.008%. The holes in the outer walls through which the wires pass were sealed. The column was placed in a temperature-controlled cabinet. The settled bed height is 300 mm.

At 10, 100, 190, and 300 mm above the support plate, pressure fluctuations were measured using Kistler piezo-electric pressure transducers. The sensors are connected by 500 mm Teflon tubes (tips flush

Brought to you by | Bibliotheek TU Delft
Authenticated | 172.16.1.226
Download Date | 8/14/12 8:51 AM

with the sidewalls); this results in a total dead volume of sensor and probe of 7500 mm^3. Again, such probes will not distort the pressure fluctuations (Van Ommen et al., 1999).

An LMS SCADAS III system is used for data acquisition. This system samples the measuring probes and provides the source signal for the Trek high-voltage power source. The potential generated by the HV source is sinusoidal, with a mean of zero. The frequencies range from 0.5 to 100 Hz. The measured time series consist of 102,400 points sampled at 400 Hz (approximately 4.25 minutes).

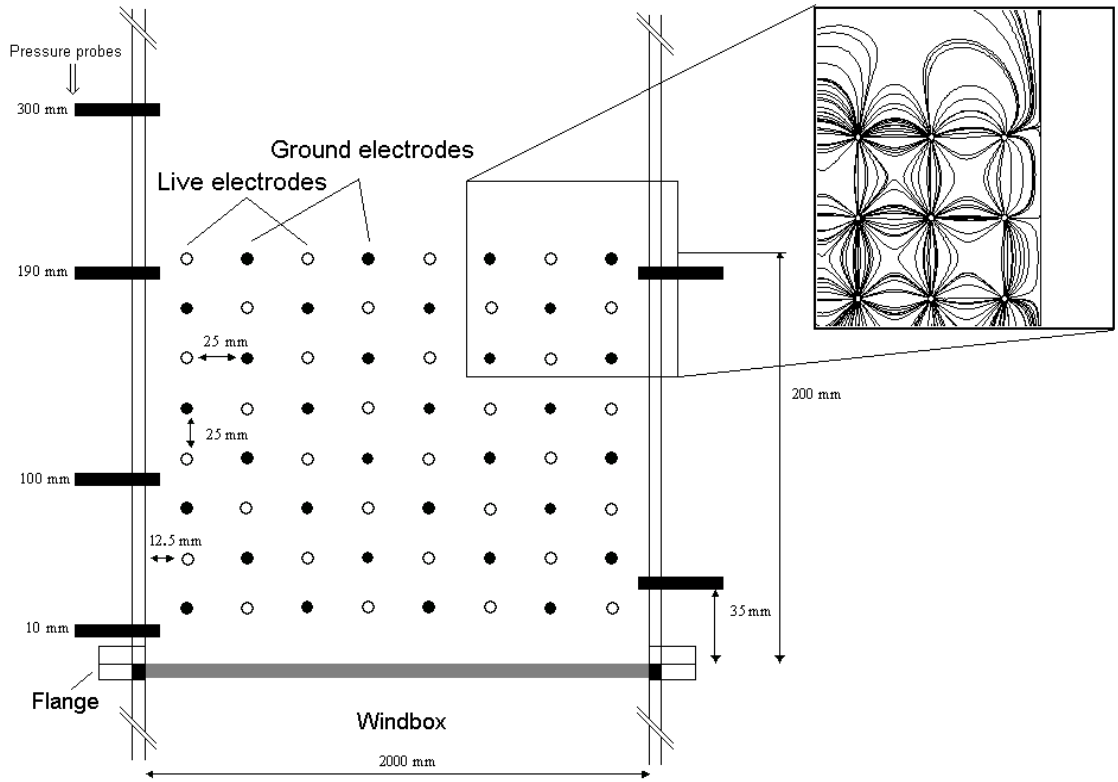

Figure 3. 2-D column design, inset depicts the quadrupole-like electric fields between the electrodes. Open circles represent live electrodes, while closed dots represent grounded electrodes. The positions of the pressure probes are also indicated.

4.3 Bubble Size Reduction in a 3-D Column by Electric Fields

The design of the 3-D column (Figure 4) is similar to the 2-D column with electrodes, albeit that for practical reasons the electrodes are now so situated that the field is purely co-flow (vertical field lines). This implies that although the electrode wires are again located inside the column, the horizontally alternating electrode pattern depicted in Figure 3 is no longer present. The horizontal external field component is therefore absent. The cylindrical system consists of a Plexiglas inner column, i.d. 80 mm. At eight levels (i.e. 12.5 mm, 25 mm, etc. of the column height) a continuous wire is strung, creating a grating-like pattern of wire with a spacing of 10 mm. The electrode grating on the next level is rotated by 90˚ (cf. Figure 4 top view). Each electrode grating thus runs crosswise to its nearest neighbors. The total height of the electrode section is 100 mm. The volume density of the electrodes is approximately 0.004%. For safety reasons, the wired inner column was placed in a Plexiglas outer column.

Pressure fluctuation sensors were installed in the wind box and at 20, 70, and 120 mm above the porous bed support. The measurement and data acquisition part of the setup is identical to the previously described 200 × 15 mm^2 2-D column, with the exception of the electrical power source. The frequencies that could be applied were limited to 1, 2, and 3.3 Hz square waves, and 50 Hz sine waves.

Brought to you by | Bibliotheek TU Delft
Authenticated | 172.16.1.226
Download Date | 8/14/12 8:51 AM

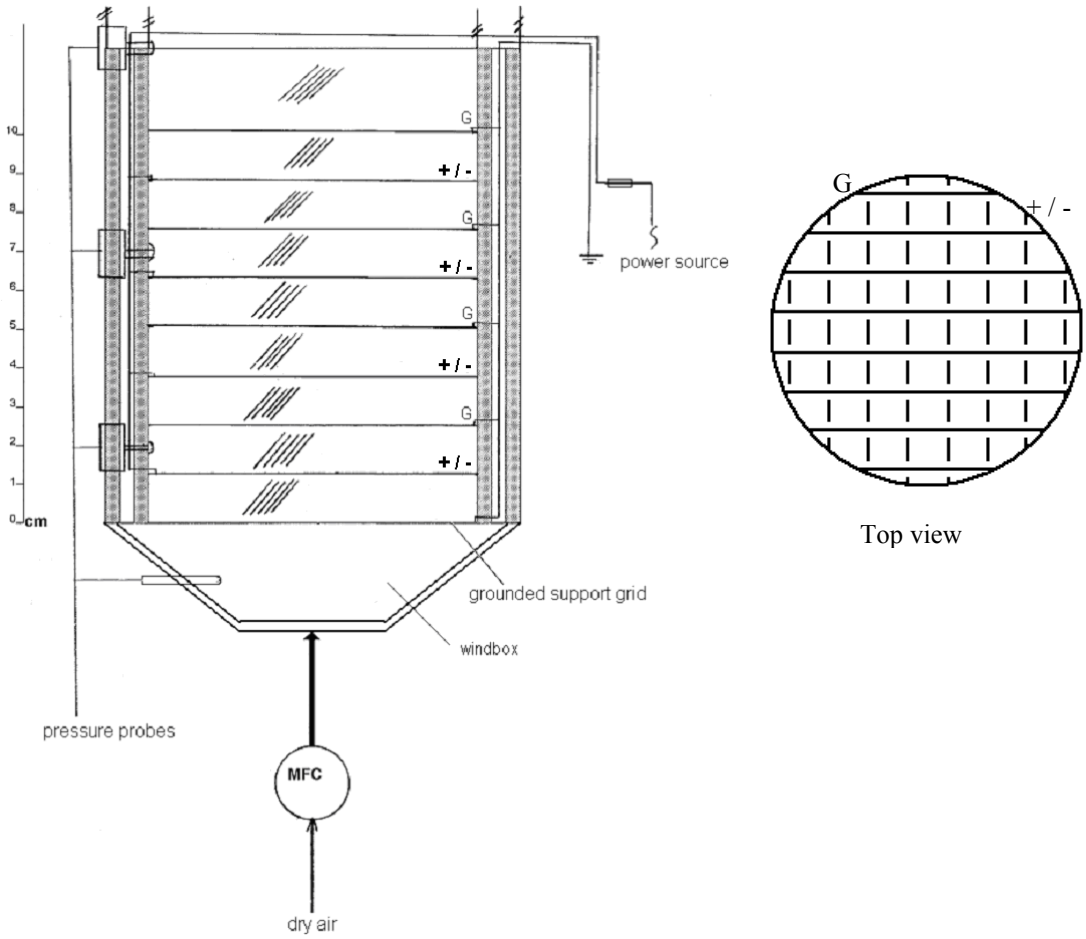

Figure 4. Side view of the 3-D column showing electrodes and pressure probe connection points. The top view depicts the intercrossing of two of the eight electrode-gratings, one of which is connected to the HV-supply, while the other is grounded.

4.4 Particle Properties

We took two types of particles for the experiments conducted in the 400 × 15 mm^2 column, to validate the relation between bubble diameters and pressure fluctuations:

- Mono-disperse glass beads, diameter d_p = 77 μm, minimum fluidization velocity U_{mf} = 1.0 cm/s. This powder is classified as Geldart A material.
- Sand, diameter range d_p = 200 – 400 μm, U_{mf} = 11.0 cm/s. This is Geldart B material.

For the electric field experiments, two types of glass beads were chosen:

- Mono-disperse glass beads, diameter d_p = 77 μm, U_{mf} = 1.0 cm/s, same as for the experiments above. The relative dielectric constant of settled bulk material was determined in a dielectric cell to be k_b = 7 at low frequencies.
- Mono-disperse glass beads, diameter d_p = 700 μm, U_{mf} = 33 cm/s, this is Geldart B material. The bulk dielectric constant, k_b, for this material is 3. This material was not used in the 3-D experiments.

Brought to you by | Bibliotheek TU Delft
Authenticated | 172.16.1.226
Download Date | 8/14/12 8:51 AM

5. RESULTS AND DISCUSSION

5.1 Measuring Pressure Fluctuations to Determine Bubble Size

The measurement of pressure fluctuations is an attractive method to characterize the hydrodynamic behavior of a fluidized bed because it is virtually non-intrusive and applicable in industrial situations. The pressure fluctuations can be measured using the probes described in the experimental section, in a manner that causes minimal disturbance of the hydrodynamic behavior. In our case, we are especially interested in the bubble characteristics, and the pressure fluctuations associated with the rising of bubbles through a fluidized bed provide an indirect measurement of their size and velocity. However, the pressure fluctuations are not only caused by the bubbles themselves – the phenomenon we are interested in – but also by other sources such as the formation, coalescence, and eruption of bubbles.

A technique proposed by Van der Schaaf et al. (2002) was used to decompose the pressure fluctuation time series in its different components. They used the coherence between two time series measured at different heights in the fluidized bed to distinguish between the different components of the pressure signals. Bubble coalescence, gas flow fluctuations, bubble eruption, and bed mass oscillations generate a fluctuation in gas velocity, which produces pressure waves that are measured almost simultaneously throughout the entire bed. These signals are therefore *coherent*. However, the gas bubbles rising through the bed cause local fluctuations in pressure, and are not measured along the entire column. These fluctuations are *incoherent*. Using a spectral decomposition technique, the incoherent power spectral density is calculated, and subsequently the corresponding incoherent standard deviation, σ_i, is determined.

As gas bubbles rise through a fluidized bed, they create pressure fluctuations with an amplitude directly proportional to their diameter (Davidson and Harrison, 1963); this can be expressed in an incoherent standard deviation, σ_i. This standard deviation is proportional to the amplitude of the fluctuation, and is a characteristic length scale (L_I) of the bubble diameter:

$$\frac{\sigma_i}{\rho_s g(1-\varepsilon_{mf})} = L_I \approx F \cdot D_b \qquad (1)$$

By measuring the pressure fluctuations at two bed heights, decomposing these in a coherent and an incoherent part, representing fast waves and bubble phenomena respectively, and examining the incoherent standard deviation, the characteristic length scales of bubbles can be ascertained. This length scale is proportional to the bubble diameter D_b. F is a constant, which is independent of bed height and superficial gas velocity. Typically, the measurements from the wind box are compared to the height under consideration. If the support plate distorts the signal too much, for example due to a high pressure drop, the measurements from within the bed just above the support plate can be used. In the results given in this paper, the incoherent power spectral density is always determined relative to the wind box signal.

Van der Schaaf et al. showed that the above method holds in a three-dimensional column (0.385m diameter, sand particles) by comparing the Darton bubble diameters (Darton, 1977) to the diameters derived from pressure fluctuations, but they did not present any direct experimental evidence. In the experiments in the 400x150 mm^2 2-D column, we used a digital video camera to verify the relation between pressure fluctuations and bubble size. The results are plotted over a range of fluidization velocities for two bed materials in Figure 5, both at a height of 600 mm (settled bed height H_b = 800 mm). Figure 5A presents the results for Geldart A glass beads. For these particles, the proportionality constant F between the bubble diameters determined from video analysis or the Darton relation and the characteristic length determined from the pressure fluctuations is ca. 8.1. For the Geldart B material (cf. Figure 5b), the proportionality factor is ca. 1.3.

Brought to you by | Bibliotheek TU Delft
Authenticated | 172.16.1.226
Download Date | 8/14/12 8:51 AM

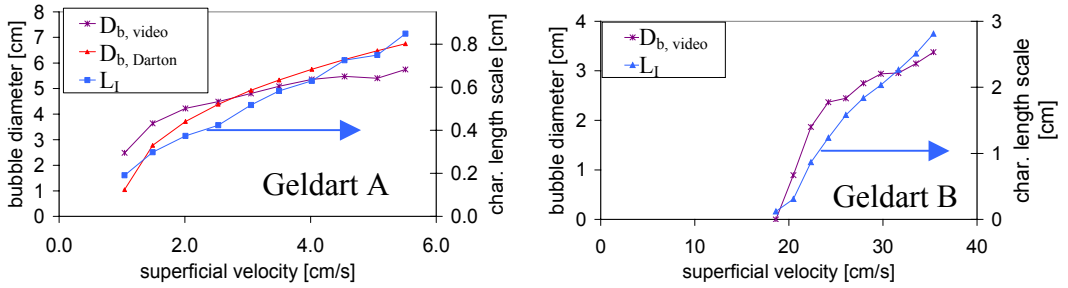

Figure 5. Comparison between mean bubble diameter determined by pressure fluctuation analysis, at 75% of the bed height, and video and Darton diameters. Left vertical axes show the arithmetic mean bubble diameter obtained from the video analysis (video: $D_{b,video}$) and the calculated (Darton relation: $D_{b,Darton}$) bubble diameter. The vertical axes on the right show the characteristic length scale calculated from the pressure fluctuations (L_I). The data in Figure 5A were gathered from fluidization of Geldart A glass beads; the 5B data are from the fluidization of Geldart B sand.

The video image analysis was sensitive enough to detect bubbles smaller than the column depth (15 mm) as well as larger bubbles – the cutoff size is 7.5 mm. However, in this method we overestimate the size of the smaller bubbles. In addition, it appears that the Darton relation for bubble diameters holds well for the Geldart A material, but the fact that we are analyzing bubbles in a flat 2-D column plays a much greater role for the bubbles in Geldart B material. The Darton bubble diameters for Geldart B particles are much larger, and not shown in the figure.

From these and other results it can be concluded that the bubble diameter calculated from the incoherent standard deviation correspond well to that determined by video analysis. The proportionality constant F is a constant for a given bed material and a range of velocities and measuring heights, but cannot yet be predicted for various bed materials.

5.2 Bubble Size Reduction in a 2-D Column by Electric Fields

The effectiveness of electric fields on the bubbling behavior in the electrically wired columns can be evaluated using the quantitative correlation between pressure fluctuations and bubble size established in section 5.1. Because the exact values of the proportionality constant, F, are not known, all results are given as a decrease in percent or fraction of the bubble diameter for the situation without electric field. The experiments were all performed in the 200 × 15mm^2 column using sinusoidal AC fields of varying frequency and strength.

The results of two different bed materials are shown in the color plots of Figs. 6 and 7. Figure 6 shows the impact of the electric field on the Geldart A material, the 77 μm glass beads. The results represent data for a gas flow of three times the minimum fluidization velocity. Bed expansion during fluidization with and without electric field was visually observed to be very similar, and fluidity (particle movement) was conserved. However, the fact that the bed expansion is not changed does not mean that the bubble behavior remains unchanged. In fact it changes considerably, as we could prove by our pressure fluctuation analysis. The reduction in bubble diameter at the measuring height shown is about 25% compared to the blank experiments. This corresponds to a decrease in bubble volume (assuming spherical bubbles) of approximately 60%. In view of the drop in total bubble volume, we speculate that the interstitial gas flow is increased. Further experiments will be carried out to check this.

Brought to you by | Bibliotheek TU Delft
Authenticated | 172.16.1.226
Download Date | 8/14/12 8:51 AM

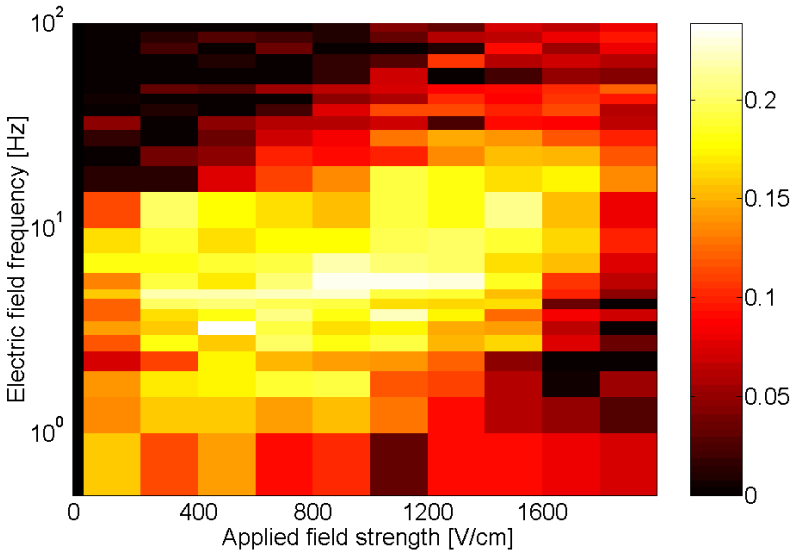

Figure 6. Color plot of bubble size decrease at 190 mm (63% of bed height) as a function of frequency and applied field. The color scale displays the decrease as a fraction of the mean bubble diameter for the situation without field i.e. before and after application of the external field. Bed material: 77 μm glass beads. The optimal working region is the yellow one, in which the decrease amounts to about 25%.

From Figure 6 it is also clear that an optimal regime of electric fields exists: the applied fields should range from 400 to 2000 V/cm, although an effect is observed even at low field strengths. The frequencies are most optimal between 5 and 20 Hz. The limits seen on the frequency range can be understood in a qualitative manner: at low frequencies, the bed characteristics change to a DC-like behavior, eventually resulting in compaction and agglomeration. This leads to a (partially) frozen bed. At high frequencies, there is not enough time for the macroscopic charge separation to develop – confer the relaxation times listed by Colver (2000). At the lower voltage limit, the electric interparticle forces are too small to play a role in the bubble behavior. At too high field strengths, it is likely that the particles stick together too strongly, resulting in more cohesive fluidization with its associated gas voids.

Similar experiments were conducted for larger glass beads (d_p=700 μm). For these Geldart B particles bubbling behavior is much more pronounced, and homogeneous fluidization is not a standard feature. The flow rate was 1.5 × U_{mf}. It was confirmed visually that fluidization was maintained throughout the experiment. The results show a much larger decrease in incoherent standard deviations than for the smaller particles, up to 85% as compared to the zero-field situation. Again an optimal frequency range of 20 to 70 Hz emerges, although less pronounced than in the Geldart A experiments. Still a strong dependence on the frequency and voltage combination is evident. The stronger tendency of the Geldart B particles to bubble is responsible for the shift to higher fields. Contrary to the experiments with finer particles, no bubble size reduction is noticed at low field strengths in these experiments.

Brought to you by | Bibliotheek TU Delft
Authenticated | 172.16.1.226
Download Date | 8/14/12 8:51 AM

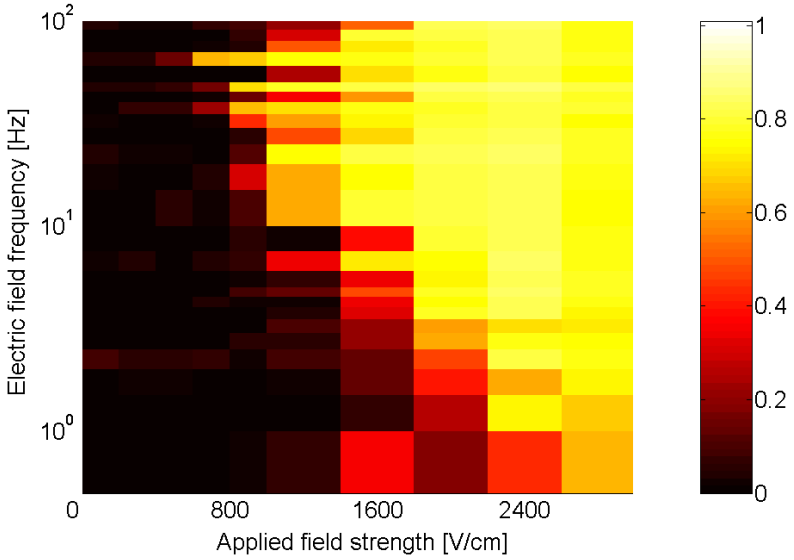

Figure 7. Color plot of bubble size decrease at 190 mm (63% of bed height), as function of frequency and applied field. Bed material: 700 μm glass beads. Note that the color scale range now extends to a fraction of 1 of the bubble size at zero field. The optimal region, in which the decrease goes up to 0.8 or 80%, is again colored yellow.

5.3 Bubble Size Reduction in a 3-D Column by Electric Fields

In the 3-D column the direction of the electric field is different from the 2-D design due to practical limitations. The applied AC-field between all 90°-to- 90° stacked gratings or electrode layers is directed up- and downward, as can be seen from Figure 4. In addition, the electric field frequencies were limited to square waves of 1, 2, and 3.3 Hz, and sine waves of 50 Hz. The top electrode is located at 71% of the settled bed height.

Results are shown at the same flow velocity as the 2-D experiments with Geldart A particles: $3 \times U_{mf}$. The preference for slowly oscillating frequencies is clearly demonstrated (Figure 8A). In addition, an optimal voltage range is again observed, at various heights in the column (Figure 8B). The decrease in bubble size is comparable to that measured in the 2-D experiments. It is interesting to note that the drop in bubble diameter as a function of frequency in the 3-D column does not show the maximum seen in the 2-D experiments. A likely explanation is that the low frequency (1, 2, and 3.3 Hz) fields in the 3-D experiments are square waves – therefore, a period of relaxation of the interparticle force basically does not exist, allowing little time for the particles to separate. This in turn is not beneficial to the fluidity of the bed.

Experiments to compare the effect of square wave alternating fields with sinusoidal ones will be carried out in the near future. We also plan to investigate the frequency and field dependence in a 3-D column in more detail.

Brought to you by | Bibliotheek TU Delft
Authenticated | 172.16.1.226
Download Date | 8/14/12 8:51 AM

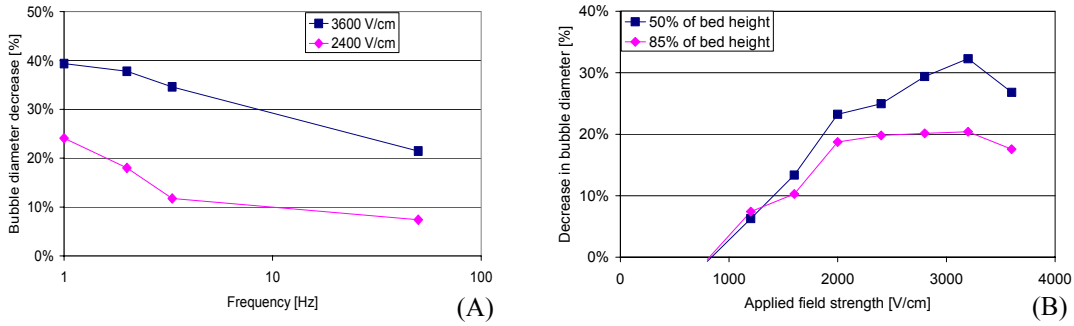

Figure 8. A. Frequency dependence of bubble decrease in the 3-D column, measured at 50% of the bed height. B. Field strength dependence in the 3-D column, with 3.3 Hz block waves. The measurements were done at 50 and 85% of bed height.

6. Conclusions

We showed that the use of electric fields yields a significant bubble reduction. In order to maintain smooth fluidization, co-flow AC-fields with a relatively low frequency are optimal. The literature review showed that DC fields, on the other hand, tend to inhibit the free movement of particles and result in a build-up of particles on the electrodes.

The mechanism of polarization is related to that found in electrorheology. In this field, as well as in fluidization experiments, it was observed that the field frequency affects the strength of the dipole moment, suggesting that the surface conductivity is the dominant factor in the interfacial Maxwell-Wagner polarization of the particle. In addition, the strength of the interparticle force depends strongly on the interparticle distance, and is relatively stronger for smaller than for larger particles. For Geldart A particles, the electric force is comparable to the drag and gravity forces. For the larger Geldart B particles, drag and gravity forces quickly exceed the electrical forces. However, because the drag and gravity forces balance each other, small forces can still play a significant role in the fluidization of larger particles.

Time series analysis of pressure fluctuations was explored to quantify the changes in bubble size. By comparing the time series measured simultaneously in the wind box and in the fluidized bed, a characteristic length scale for the bubble diameter could be derived. This technique, proposed by Van der Schaaf et al. (2002), was tested in a 2-D column using video image analysis. It was found that the bubble diameter is proportional to the incoherent standard deviation at the range of fluidization velocities and measuring heights studied, but that the proportionality factor depends on the type of material being fluidized. The influence of the dimensions of the column was not investigated.

By invoking the pressure fluctuation analysis, a marked reduction in bubble size was found in both 2-D and 3-D columns with electrodes. For 77 μm particles, it turned out that bubble diameters could be decreased by 25-35%, both in 2-D and 3-D columns. The reduction in bubble diameter when larger particles are fluidized is even more dramatic, up to 85%. The use of sinusoidal, low frequency fields allows particle movement, and thus the state of fluidization, to be preserved – an improvement over much of the earlier work. The optimal frequency differs for the different particle sizes – approximately 5-20 Hz for small particles, to 20-70 Hz for particles with a diameter of 700 μm. The bed height was seen to change very little upon applying the electric fields, despite the fact that the average bubble volume becomes much smaller. Future work will be conducted to find out whether the total bubble volume is decreased likewise.

Brought to you by | Bibliotheek TU Delft
Authenticated | 172.16.1.226
Download Date | 8/14/12 8:51 AM

Notation

d_p	particle diameter, m
D_b	bubble diameter, m
F	proportionality constant, -
g	gravitational acceleration, m/s^{-2}
H_b	settled bed height, m
k_b	dielectric constant of bulk material, -
k_p	dielectric constant of particle, -
L_I	characteristic length scale derived from pressure fluctuation analysis, m
U	superficial velocity, m/s
U_{mf}	minimum fluidization velocity, m/s
ΔP	pressure drop, mbar
ε_{mf}	bed porosity at minimum fluidization conditions, -
ρ_s	solids density, kg/m^3
σ_i	incoherent standard deviation, Pa

References

Chen, Y., Sprecher, A.F., and Conrad, H., "Electrostatic particle-particle interactions in electrorheological fluids", J. Appl. Phys., Vol. 70, 6796-6803 (1991).

Colver, G.M., "Bubble control in gas-fluidized beds with applied electric fields", Powder Technol., Vol. 17, 9-18 (1977).

Colver, G.M., "An interparticle force model for ac-dc electric fields in powders", Powder Technol., Vol. 112, 126-136 (2000).

Coppens, M.-O. "Method for operating a chemical and/or physical process by means of a hierarchical fluid injection system", US Patent 6333019 (2001).

Darton, R.C., LaNauze, R.D., Davidson, J.F., and Harrison, D., "Bubble growth due to coalescence in fluidised beds", Trans. Inst. Chem. Eng., Vol. 55, 274-280 (1977).

Davidson, J.F., and Harrison, D., *"Fluidized Particles"*, Cambridge Univ. Press, Cambridge (1963).

Dietz, P.W., and Melcher, J.R. "Interparticle electrical forces in packed and fluidized beds", Ind. Eng. Chem. Fundam., Vol. 17, No. 1, 28-32 (1978).

DIPImage image analysis software, Pattern Recognition Group, Department of Applied Physics, Delft University of Technology.

Elsdon, R., and Shearer, C.J., "Heat transfer in a gas fluidized bed assisted by an alternating electric field", Chem. Eng. Sci., Vol. 32, 1147-1153 (1977).

Geuzens, P.L., "Some Aspects of Magnetically Stabilized Fluidization", PhD-thesis, Technical University of Eindhoven, The Netherlands (1985).

Hristov, J., "Magnetic field assisted fluidization – a unified approach: a series of review papers", Rev. Chem. Eng., Vol. 18, Nos. 4-5 (2002).

Johnson, T.W., and Melcher, J.R., "Electromechanics of electrofluidized beds", Ind. Eng. Chem., Fundam., Vol. 14, No. 3, 146-153 (1975).

Jones, T.B. "*Electromechanics of Particles*." Cambridge University Press, Cambridge, 1995.

Brought to you by | Bibliotheek TU Delft
Authenticated | 172.16.1.226
Download Date | 8/14/12 8:51 AM

Kaart, S., "Controlling Chaotic Bubbles", PhD-thesis, Delft University of Technology (2002).

Katz, H., "Method of stabilizing a fluidized bed using a glow discharge", U.S. Patent 3304249 (1967).

Kwauk, M., "*Fluidization: Idealized and Bubbleless, with Applications*", Science Press, Beijing, (1992).

Levenspiel, O., "G/S reactor models – packed beds, bubbling fluidized beds, turbulent fluidized beds and circulating (fast) fluidized beds", Powder Technol., Vol. 112, 1-9 (2002).

Moissis, A.A., and Zahn, M., Conf. Record 1986 IEEE Industry Applications Soc. Annual Meeting, Part II, pg 1396-1403 (1986).

Parthasarathy, M., and Klingenberg, D.J., "Electrorheology: mechanisms and models", Mater. Sci.Eng., R17, 57-103 (1996).

Rosensweig, R.E., "Process concepts using field-stabilized two-phase flow", J. Electrost., Vol. 34, 163-187 (1995).

Seville, J.P.K., Willett, C.D., and Knight, P.C., "Interparticle forces in fluidisation: a review", Powder Technol., Vol. 113, 261-268 (2000).

Van Ommen, J.R., Schouten, J.C., Vander Stappen, M.L.M., Van den Bleek, C.M., "Response characteristics of probe-transducer systems for pressure measurements in gas-solid fluidized beds: how to prevent pitfalls in dynamic pressure measurements", Powder Technol., Vol. 106, 199-218 (1999). Erratum: Powder Technol., Vol. 113, 217 (2000).

Van der Schaaf, J., Schouten, C.C., Johnsson, F., Van den Bleek, C.M., "Non-intrusive determination of bubble and slug length scales in fluidized beds by decomposition of the power spectral density of pressure time series", Int. J. Multiphase Flow, Vol. 28, 865-880 (2002).

Wittmann, C.V., and Ademoyega, B.O., "Hydrodynamic changes and chemical reaction in a transparent two-dimensional cross-flow electrofluidized bed. 1. Experimental results", Ind. Eng. Chem. Res., Vol. 26, 1586-1593 (1987).

Wittmann, C.V., "Hydrodynamic changes and chemical reaction in a transparent two-dimensional cross-flow electrofluidized bed. 2. Theoretical results", Ind. Eng. Chem. Res., Vol 28, 454-470 (1989).

Zahn, M., and Rhee, S-W, "Electric field effects on the equilibrium and small signal stabilization of electrofluidized beds", IEEE Trans. Ind. Appl., Vol. IA-20, No.1, 137-147 (1984).

Brought to you by | Bibliotheek TU Delft
Authenticated | 172.16.1.226
Download Date | 8/14/12 8:51 AM